ISSN 0023-1584, Kinetics and Catalysis, 2010, Vol. 51, No. 5, pp. 714–723. © Pleiades Publishing, Ltd., 2010.
Original Russian Text © N.I. Skripov, L.B. Belykh, L.N. Belonogova, V.A. Umanets, E.N. Ryzhkovich, F.K. Schmidt, 2010, published in Kinetika i Kataliz, 2010, Vol. 51, No. 5, pp. 739–749.

Effect of the Nature of the Acido Ligand in the Precursor on the Properties of Nanosized Palladium-Based Hydrogenation Catalysts Modified with Elemental Phosphorus

N. I. Skripov, L. B. Belykh, L. N. Belonogova, V. A. Umanets, E. N. Ryzhkovich, and F. K. Schmidt

Irkutsk State University, Irkutsk, 664033 Russia

e-mail: belykh@chem.isu.ru

Received March 4, 2009

Abstract—The effect of the nature of the acido ligand in the precursor and the modifying action of elemental phosphorus on palladium catalysts for hydrogenation are reported. The large turnover frequency (TOF) and turnover number (TON) values observed for styrene hydrogenation on the Pd blacks prepared in situ by $PdCl_2$ reduction with hydrogen in DMF are due to the formation of fine-particle catalyst with a base particle size of 6–10 nm. This is explained by the high $PdCl_2$ reduction rate and by the formation of a palladium cluster stabilizer—dimethylammonium chloride—in the reaction system via the catalytic hydrolysis of the solvent (DMF). The modifying action of elemental phosphorus on the properties of the palladium catalysts depends on the nature of the acido ligand in the precursor. In the case of oxygen-containing precursors at small P/Pd ratios, elemental phosphorus exerts a promoting effect, raising the TON and TOF values by a factor of about 9. In the case of palladium dichloride as the precursor, white phosphorus exerts an inhibiting effect. At the same time, it enhances the stability of the catalyst, raising the TON value at P/Pd = 0.3. The causes of these distinctions are considered.

DOI: 10.1134/S0023158410050137

The problem of catalyst formation and modification has been the subject of many works [1–6]. Obviously, the nature of the modifying effect is catalyst-specific. Although the basic methods of obtaining catalysts for various processes are rather well understood, the general principles of formation of catalysts with optimum activity, selectivity, and productivity have not been formulated as yet. The main difficulty here is that a finely dispersed metal in the liquid phase or on a support is a complicated physicochemical system in which the metal is usually in different oxidation states, its surface atoms show nonuniform coordination and energetic properties, its particles are polydisperse and are bound to the support or ligand to different extents, and so on. The most rational approach to the modification problem is through investigation of the chemical aspects of catalyst formation in order to gain the deepest possible insight into all stages of the chemical reactions involved in catalyst preparation and in catalyst functioning in a given process.

Earlier, we demonstrated for the first time that elemental phosphorus can promote high-efficiency nanosized palladium catalysts for hydrogenation [7]. However, it was found that its modifying effect depends very strongly on the nature of the reducing agent and acido ligand in the precursor. Here, we report the influence of the acido ligand in the precursor on the properties of palladium-based hydrogenation catalysts modified with elemental phosphorus and formed under the action of molecular hydrogen.

EXPERIMENTAL

Solvents (benzene and *N*,*N*-dimethylformamide (DMF)) were purified by standard methods [8]. For dehydration and amine removal, DMF was held over anhydrous copper sulfate until the formation of a green solution and was distilled twice in vacuo (8 Torr) at a temperature not higher than 42°C. For deeper dehydration, benzene was additionally distilled from $LiAlH_4$ in a fractional distillation column. Purified benzene was stored in an argon atmosphere over molecular sieve 4A in sealed tubes. As determined by the Fischer method [9], the water content of benzene was 1.1×10^{-3} mol/l and that of DMF was 0.8 mol/l.

Palladium bisacetylacetonate was synthesized via the procedure described in [10]. The following ^1H NMR data were obtained for the product in benzene: $\delta(CH) = 5.04$ ppm (s, 1H), $\delta(CH_3) = 1.76$ ppm (s, 6H). Palladium diacetate and palladium dichloride (pure grade) were used as received.

White phosphorus was mechanically purified from surface oxidation products and was washed with dehydrated benzene immediately before use. A benzene solution of white phosphorus was prepared and stored in an inert atmosphere in a finger-shaped vessel whose

design allowed it to be vacuumized and filled with argon. ^{31}P NMR data: $\delta = -522$ ppm (s).

The reaction between palladium dichloride and white phosphorus was carried out in an inert atmosphere at different component ratios in a finger-shaped vessel. In the reactant ratios specified below, phosphorus is accepted to be in atomic form.

Example 1. $PdCl_2$ (0.3552 g, 2.0 mmol) in 125 ml of DMF was added to 2 ml of a benzene solution of white phosphorus (0.6 mmol) vigorously stirred with a magnetic stirrer. At the instant the reactants were combined, the color of the solution changed from yellowish orange to intense black. The hydrochloric acid concentration in DMF was determined by potentiometric titration with a KOH solution using a pH-410 millivoltmeter and an ESLK-01.7 laboratory glass combination electrode. Phosphorus conversion products were identified by ^{31}P NMR spectroscopy. After 5 h, the solution was concentrated in vacuo (40°C, 1 Torr) to 1/5 of its initial volume, and 10 ml of benzene was added. The resulting black precipitate was filtered, washed with benzene three times, and dried in vacuo (30°C, 1 Torr). The product yield was 0.1 g (sample 1).

The X-ray powder diffraction pattern of sample 1 showed reflections from unreacted palladium dichloride crystals and a diffuse halo at $2\theta = 35°–45°$. This range of diffraction angles accommodates the strongest peaks of palladium metal and palladium phosphides. The coherent-scattering domain (CSD) size calculated using the Selyakov–Scherrer formula [11] was 2.8 nm. In order to bring the solid into the crystalline state and gain additional information concerning the product composition, sample 1 was heat-treated at 400°C in a sealed tube in an inert atmosphere for 4 h and was then cooled slowly. Part of sample 1 sublimated during the heat treatment to yield a white powder, and a black powder remained on the bottom of the tube.

The X-ray diffraction pattern of the unsublimated part of sample 1 (black powder) showed the following reflections ($d/n(I/I_0)$): 2.985(5), 2.778(3), 2.738(6), 2.714(5), 2.693(17), 2.585(11), 2.562(19), 2.508(3), 2.439(10), 2.359(30), 2.328(19), 2.299(49), 2.254(100), 2.238(34), 2.216(37), 2.121(14), 2.102(20), 2.032(21), 2.014(6), 1.997(28), 1.953(5), 1.907(6), 1.889(5), 1.862(11), 1.845(9), 1.802(3), 1.784(3), 1.731(3), 1.682(1), 1.615(2), 1.579(2), 1.569(4), 1.543(2), 1.511(4), 1.456(7), 1.432(3), 1.409(10), 1.378(6), 1.346(11), 1.331(8), 1.310(3), 1.290(6), and 1.281(4) Å (hereafter, the numbers in parentheses are relative peak intensities).

The reflections at 2.985, 2.714, 2.562, 2.359, 2.299, 2.254, 2.238, 2.216, 2.121, 2.032, 2.014, 1.907, 1.889, 1.862, 1.845, 1.784, 1.731, 1.569, 1.543, 1.456, 1.409, 1.346, 1.331, 1.290, and 1.281 Å are in good agreement with the standard X-ray diffraction data for the palladium phosphide Pd_6P (PDF 19-882) [12]. The reflections at 2.738, 2.714, 2.508, 2.439, 2.328, 2.254, 2.216, 2.121, 2.102, 1.997, 1.953, 1.845, 1.731, 1.682, 1.432, 1.378, 1.346, and 1.290 Å are from the palladium phosphide Pd_5P_2 (PDF 19-887) [11]. Finally, the reflections at 2.693, 2.439, 2.359, 2.254, 2.121, 2.102, 1.997, 1.907, 1.889, 1.862, 1.802, 1.682, 1.615, 1.511, 1.378, 1.331, 1.310, and 1.290 Å are due to the palladium phosphide Pd_3P [13]. The peaks at 2.778, 2.585, and 1.579 Å were not assigned to any phase.

The diffraction pattern of the sublimated part of sample 1 (white powder) exhibited reflections at 3.875(16), 3.745(100), 2.237(9), 1.938(12), 1.736(7), 1.583(16), 1.370(4), 1.290(3), and 1.226(4) Å. All of them coincide with the standard X-ray diffraction data for NH_4Cl (PDF 7-7) [12].

The syntheses at other P/Pd ratios in an argon atmosphere were carried out in the same way. The product yield from the reaction between palladium dichloride and elemental phosphorus was 0.3505 g for P/Pd = 1 (sample 2) and 0.3880 g for P/Pd = 3 (sample 3). Samples 2 and 3 were X-ray-amorphous. As the products of the reaction between palladium dichloride and white phosphorus were crystallized in an argon or hydrogen atmosphere, there was always ammonium chloride sublimation from the sample.

The X-ray diffraction data for the unsublimated part of sample 2 (P/Pd = 1, black powder) are as follows ($d/n(I/I_0)$): 2.769(19), 2.728(21), 2.690(48), 2.577(41), 2.438(63), 2.368(69), 2.327(81), 2.282(34), 2.254(84), 2.322(100), 2.118(83), 2.091(49), 1.994(30), 1.901(24), 1.888(10), 1.858(37), 1.800(9), 1.728(6), 1.613(7), 1.577(7), 1.509(19), 1.434(15), 1.409(6), 1.384(6), 1.375(15), 1.330(34), 1.301(13), 1.288(15), 1.279(14), and 1.259(15) Å. The reflections at 2.769, 2.690, 2.577, 2.438, 2.368, 2.327, 2.254, 2.232, 2.118, 2.091, 1.994, 1.901, 1.888, and 1.858 Å check with the standard X-ray diffraction data for $Pd_{4.8}P$ (PDF 19-0890) [12]; the reflections at 2.690, 2.577, 2.368, 2.327, 2.282, 2.254, 2.232, 2.118, 2.091, 1.994, 1.901, 1.888, 1.858, 1.800, 1.728, 1.577, 1.509, 1.434, 1.409, 1.375, 1.330, 1.301, 1.288, and 1.279 Å, with the standard X-ray diffraction data for $Pd_{12}P_{3.2}$ (PDF 42-0922) [12]; the reflections at 2.690, 2.438, 2.368, 2.282, 2.254, 2.118, 2.091, 1.994, 1.901, 1.888, 1.858, 1.800, 1.728, 1.613, 1.509, 1.384, 1.330, 1.301, 1.288, and 1.259 Å, with the X-ray diffraction data for Pd_3P [13]; the reflections at 2.728, 2.438, 2.282, 2.254, 2.118, 2.091, 1.858, 1.728, 1.434, 1.375, 1.330, and 1.301 Å, with the X-ray diffraction data for Pd_5P_2 [12]. The X-ray diffraction data for $Pd_{12}P_{3.2}$ and Pd_3P are similar. The palladium phosphide $Pd_{12}P_{3.2}$ is also designated $Pd_3P_{0.8}$.

As was mentioned above, sample 3 (P/Pd = 3) is also X-ray-amorphous. However, the maximum of the diffuse halo for this sample is observed at smaller angles of $2\theta = 19°–40°$. This 2θ range accommodates the strongest reflections from the palladium phosphide PdP_2: 2.928(72), 2.882(100), and 2.727(68) Å [14]. After the heat treatment of sample 3 (P/Pd = 3) at 400°C, the X-ray diffraction pattern of the unsubli-

mated residue (black powder) showed the following reflections: 3.984(80), 2.928(53), 2.880(90), 2.722(100), 2.606(17), 2.516(22), 2.495(26), 2.286(51), 2.122(34), 2.080(23), 2.052(31), 1.993(31), 1.898(22), 1.837(34), 1.793(33), 1.734(20), 1.689(17), 1.645(15), 1.489(13), 1.465(18), and 1.356(11) Å. The reflections at 2.928, 2.880, 2.722, 2.495, 2.052, 1.993, 1.898, 1.689, 1.465, and 1.356 Å are due to the palladium phosphide PdP_2 [14]. The other reflections were not assigned.

Catalytic hydrogenation was performed in a temperature-controlled glass shaker at 30°C and an initial hydrogen pressure of 1 atm in the presence of a palladium catalyst obtained in situ. The catalyst was prepared as follows. A finger-shaped vessel was vacuumized and filled with argon, and 1 ml of a benzene solution of white phosphorus was placed there. Next, 9 ml of 1.1×10^{-3} M palladium dichloride in DMF was added to this solution under flowing argon with vigorous magnetic stirring (P/Pd = 0.1–2.0). Immediately after the solutions were combined, the color of the mixture changed from yellowish orange to brownish black. The solution was stirred for 5 min at room temperature and was then transferred into a prevacuumized, hydrogen-filled, temperature-controlled shaker. The shaker was closed with a Teflon stopper with a rubber septum, a positive hydrogen pressure of 1 atm was established, and the substrate was introduced with a syringe. Hydrogenation was conducted under vigorous agitation to rule out diffusion control of the reaction. The reaction was monitored volumetrically and by GLC.

Catalytic systems based on palladium acetate were prepared in a similar way.

Catalysts based on $Pd(acac)_2$ and elemental phosphorus were prepared directly in the shaker reactor under flowing hydrogen. The reduction of $Pd(acac)_2$ was carried out at 80°C, including in the presence of phosphorus.

Example 2. A catalyst based on $PdCl_2$ and elemental phosphorus was synthesized in a hydrogen atmosphere (sample 4). A solution of $PdCl_2$ (0.3552 g, 2.0 mmol) in DMF (125 ml) was added to 6 ml of a benzene solution of 0.6 mmol of white phosphorus (P/Pd = 0.3) in an argon atmosphere under vigorous magnetic stirring. After 5 min, the resulting brownish black solution was transferred into a temperature-controlled shaker reactor under flowing hydrogen. The reaction mixture was agitated at a hydrogen pressure of 1 atm and a temperature of 30°C for 7 min. After the reaction was complete, the blackish brown solution was transferred into a finger-shaped vessel in an inert atmosphere, 2/3 of the solution was removed in vacuo, and benzene was added until the formation of a precipitate. The precipitate was washed three times with benzene and was dried in vacuo (50°C, 1 Torr). The product yield was 0.20 g. The IR spectrum of the product showed no absorption bands in the 400–4000 cm^{-1} range. The product was X-ray-amorphous. Its diffraction pattern exhibited a halo in the $2\theta = 35°–45°$ range. The CSD size was 3.4 nm.

The X-ray diffraction pattern of the unsublimated part of sample 4 (P/Pd = 0.3, black powder) showed the following reflections: 2.982(6), 2.716(5), 2.563(26), 2.383(28), 2.291(54), 2.252(100), 2.220(53), 2.109(20), 2.031(29), 2.014(12), 1.988(21), 1.948(15), 1.864(9), 1.847(10), 1.781(2), 1.569(4), 1.540(2), 1.454(8), 1.417(8), 1.405(9), 1.377(9), 1.340(14), 1.283(3), and 1.242(5) Å. The reflections at 2.982, 2.716, 2.563, 2.383, 2.291, 2.252, 2.220, 2.109, 2.031, 2.014, 1.864, 1.847, 1.781, 1.569, 1.540, 1.454, 1.417, 1.340, 1.283, 1.242, and 1.217 Å are due to the palladium phosphide Pd_6P (PDF 19-882) [12]. The reflections at 2.252, 1.948, and 1.377 Å are from crystalline palladium (PDF 5-0681) [12]. The reflections at 1.988 and 1.405 Å were not assigned.

The synthesis of a catalyst in a hydrogen atmosphere at P/Pd = 1 was carried out in a similar way (sample 5). The product yield in this case was 0.2738 g. The sample was X-ray-amorphous. The diffuse halo was observed at $2\theta = 35°–45°$. The CSD size was 1.8 nm. The X-ray diffraction pattern of the unsublimated part of sample 5 (black powder) showed the following reflections: 2.767(18), 2.696(48), 2.589(43), 2.445(59), 2.371(72), 2.330(79), 2.259(85), 2.237(100), 2.118(69), 2.092(45), 1.998(27), 1.953(5), 1.909(24), 1.892(9), 1.850(36), 1.804(6), 1.744(3), 1.680(4), 1.614(5), 1.579(6), 1.511(18), 1.489(3), 1.456(3), 1.435(12), 1.411(3), 1.387(5), 1.367(14), 1.331(33), 1.302(13), 1.280(15), 1.261(13), and 1.234(6) Å. The reflections at 2.696, 2.371, 2.330, 2.259, 2.237, 2.118, 2.092, 1.998, 1.909, 1.892, 1.850, 1.804, 1.744, 1.680, 1.614, 1.579, 1.511, 1.456, 1.435, 1.411, 1.387, 1.367, 1.331, 1.302, 1.280, 1.261, and 1.234 Å are due to $Pd_{12}P_{3.2}$ (PDF 42-922) [12]. The reflections at 2.767, 2.589, 2.445, 2.371, 2.330, 2.259, 2.237, 2.118, 2.092, 1.998, 1.909, 1.892, and 1.850 Å check well with the X-ray diffraction data for $Pd_{4.8}P$ (PDF 19-0890) [12]. The reflections at 2.259, 1.953, and 1.387 Å are due to Pd (PDF 5-0681) [12].

The Pd(0) determination procedure was described earlier [15]. Some properties of the catalysts obtained in a hydrogen atmosphere are listed in Table 1.

^{31}P NMR spectra were recorded on a VXR 500S Varian pulsed spectrometer. The chemical shifts of ^{31}P signals were measured versus 85% phosphoric acid. Positive values corresponded to downfield shifts. The solutions to be characterized by NMR were sealed in prevacuumized coaxial inserts and filled with argon.

X-ray diffraction patterns were obtained on a DRON-3M diffractometer (CuK_α radiation).

Transmission electron microscopic (TEM) images were obtained with a Philips EM-410 microscope. A drop of a catalyst solution prepared in situ was placed on a carbon-coated specimen grid and was dried in an argon atmosphere. The imaging conditions ruled out

Table 1. Characteristics of elemental phosphorus–modified hydrogenation catalysts prepared in a hydrogen atmosphere

Precursor	P/Pd	X-ray diffraction data				Pd(0) content, %
		initial sample		heat-treated sample		
		composition	CSD size, nm	composition	CSD size, nm	
$PdCl_2$	0	Pd	14	Pd, NH_4Cl	23.5	Not determined
	0.3	X-ray-amorphous	3.4	Pd (cr.), Pd_6P, NH_4Cl	–	38
	1	X-ray-amorphous	1.8	Pd (cr.), $Pd_{12}P_{3.2}$, $Pd_{4.8}P$, NH_4Cl	–	12
$Pd(acac)_2$	0	Pd	20	Not determined	–	Not determined
	0.3	X-ray-amorphous	3.1	Pd_6P	–	27
	1.0	X-ray-amorphous	2.0	Pd_5P_2, PdP_2	–	8

the melting or decomposition of the specimen under the action of the electron beam.

RESULTS AND DISCUSSION

We demonstrated earlier [6, 16] that the nanoparticles resulting from $Pd(acac)_2$ reduction with hydrogen in the presence of elemental phosphorus (P/Pd = 0.3) are highly efficient hydrogenation catalysts. Their turnover frequency (TOF) and turnover number (TON) are higher than those of Pd black prepared in situ under the same conditions by a factor of 9 and 8.6, respectively (Fig. 1). Similar data were obtained for $Pd(OAc)_2$.

Use of palladium dichloride as the precursor leads to the opposite result. Firstly, the Pd black obtained in situ by $PdCl_2$ reduction with hydrogen in DMF is characterized by fairly large TOF and TON values in styrene hydrogenation. While the activity of the Pd black prepared from $Pd(acac)_2$ or $Pd(OAc)_2$ in DMF is 30 and 60 (mol styrene) (g-at Pd)$^{-1}$ min^{-1}, respectively, the activity of the Pd black obtained from the $PdCl_2$ precursor is 190 (mol styrene) (g-at Pd)$^{-1}$ min^{-1} (Fig. 1). Secondly, when the precursor is $PdCl_2$ rather than an oxygen-containing compound, addition of elemental phosphorus lowers the catalytic activity, irrespective of the reactant ratio (Fig. 2). At the same time, the introduction of white phosphorus increases the TON value through enhancing the stability of the catalyst (Fig. 1). Thirdly, the catalyst prepared from $PdCl_2$ is absolutely inactive at larger P/Pd ratios (Fig. 2).

Since styrene hydrogenation is not a structure-sensitive reaction, the high activity of Pd black can be explained either by the increased number of active sites as a consequence of the formation of a more disperse system or by the appearance of new, more active sites. According to our ligand-dependent catalytic activity data, the Pd particle size decreases and,

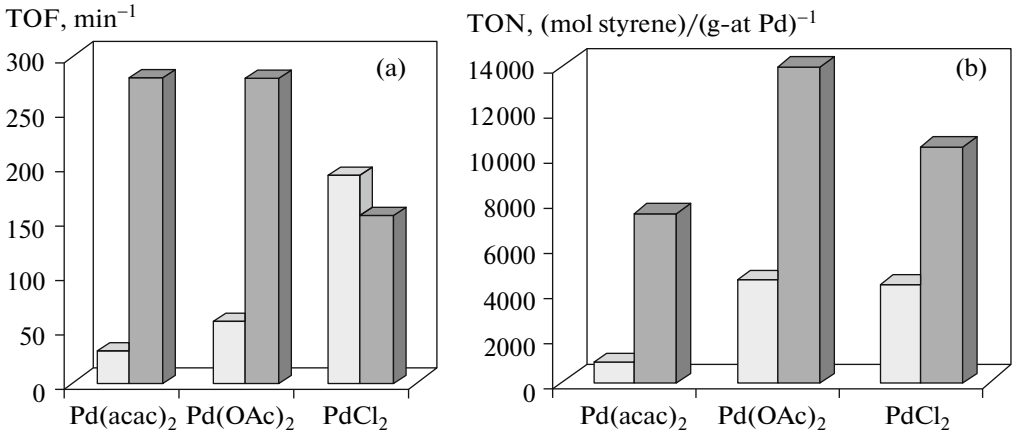

Fig. 1. (a) TOF and (b) TON for styrene hydrogenation on Pd blacks prepared in situ (light columns) and on elemental phosphorus–modified palladium catalysts (dark columns). Pd content, 1 mmol/l; P/Pd = 0.3; styrene/Pd = 870; T = 30°C; H_2 pressure, 1 atm.

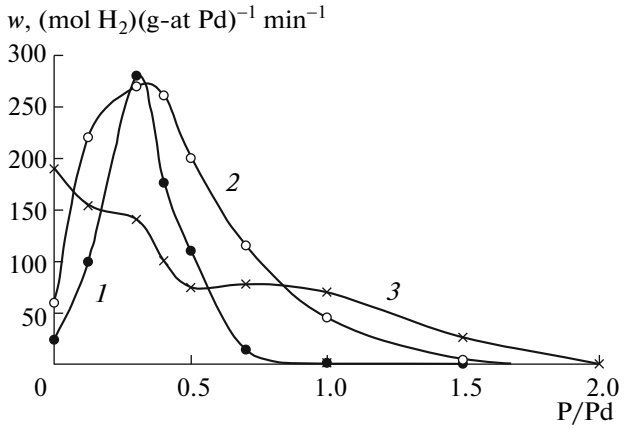

Fig. 2. Activity (w) of the palladium catalysts prepared from (*1*) $Pd(acac)_2$, (*2*) $Pd(OAc)_2$, and (*3*) $PdCl_2$ and modified with elemental phosphorus in styrene hydrogenation as a function of the reactant ratio. Pd content, 1 mmol/l; styrene/Pd = 870; DMF medium; $T = 30°C$; H_2 pressure, 1 atm.

accordingly, the degree of dispersion increases in the order acac < OAc < Cl.

As was demonstrated by TEM, the size of the base Pd black particles obtained from $Pd(acac)_2$ is 25–30 nm (Fig. 3a). These solid nanoparticles, similar in size, tightly bound with one another at their contact points, form branching chains looking like fractal clusters [17, 18]. In the Pd black prepared from $PdCl_2$, we observed fairly large high-contrast particles 50–100 nm in diameter. However, these particles were not monoliths and consisted of base particles 6–10 nm in diameter (Fig. 3b).

A similar situation is observed in the micrograph of palladium clusters obtained by K_2PdCl_4 reduction with polyoxometalates [19], which serve simultaneously as nanoparticle stabilizers. The self-organization of the base nanoclusters 6 nm in diameter yields spherical, hollow, supramolecular, blackberry-like structures 60–100 nm in size. The structuring of the base particles is attributed [19] not to the hydrophobic interaction of palladium clusters via van der Waals forces, which is typical of the formation of fractal clusters, but to the presence of soluble electrical layer on the palladium nanocluster surface. Macroanions are adsorbed by the surface and impart the palladium nanoclusters a negative charge. The counterions are attracted simultaneously to several negatively charged nanoparticle cores and thus hold them together. The formation of this kind of supramolecular structure is not unique to polyoxometalates. Such structures are typical of any nanoparticles having a suitable size and hydrophilic surface in a polar solvent [19].

The presence of two different supramolecular structures in the Pd blacks can be due to the fact that the rate-limiting steps of their formation are different. The limiting step of the formation of fractal structures both in the case of diffusion-limited aggregation and in the case of cluster–cluster aggregation is the diffusion of base particles, with the probability of sticking of primary particles being unity [17, 18]. If the rate limiting step is particle growth, then the weak sticking of the base particles to one another will favor deeper interpenetration of primary particles and the formation of more compact aggregates.

The observed difference between the sizes of the base particles of the Pd blacks arises from the difference between the precursor reduction rates. Palladium dichloride is reduced by hydrogen in DMF within 0.5–1 min even at 30°C, while the reduction of $Pd(acac)_2$ needs a temperature not lower than 60–70°C to proceed at a noticeable rate and has a short induction period.

The IR spectrum of the Pd black obtained from $PdCl_2$ has no bands in the 400–4000 cm^{-1} range. As the Pd black is heat-treated at 400°C for converting it into a crystalline phase, a small part of the sample undergoes sublimation to yield a white powder. According to X-ray diffraction data, the sublimation product is ammonium chloride. Note that the X-ray diffraction pattern of the initial Pd black sample shows no reflections from crystalline ammonium chloride. Therefore, either NH_4Cl results from the heat treatment of the sample or this salt or its precursor is in a finely dispersed state and is X-ray-amorphous.

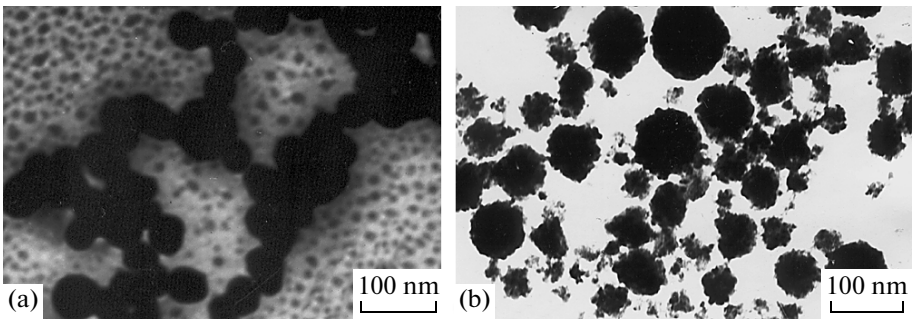

Fig. 3. TEM images of the Pd blacks obtained by the reduction of palladium compounds with hydrogen in the DMF medium (palladium content of 1 mmol/l, H_2 pressure of 1 atm): (a) $Pd(acac)_2$ precursor, 80°C; (b) $PdCl_2$ precursor, 30°C.

The identification of ammonium chloride among the reaction products might seem unexpected. However, amides of carboxylic acids can undergo hydrolysis, which is accelerated by both strong mineral acids and bases [20], and salts of ammonium and substituted ammonium bases, as well as the amines resulting from their decomposition, are thermally unstable. In particular, tertiary, secondary, and primary amines are unstable at 200–300°C and undergo destruction in the presence of HCl with stepwise N–C bond breaking [21]. Although DMF was dried, it retained some water, whose concentration was 0.8 mol/l, and palladium dichloride hydrogenolysis yielded HCl, a strong acid. As a consequence the formation of Pd black could be accompanied by the catalytic hydrolysis of DMF with the formation of dimethylammonium chloride:

$$PdCl_2 + H_2 = Pd(0) + 2HCl,$$

$$HC(O)N(CH_3)_2 + H_2O \xrightarrow{HCl} HCOOH + NH(CH_3)_2,$$

$$HN(CH_3)_2 + HCl = [NH_2(CH_3)_2]Cl.$$

The thermal decomposition of dimethylammonium chloride yielded ammonium chloride:

$$HN(CH_3)_2 + HCl \xrightarrow{200–300°C} NH_2CH_3 + CH_3Cl,$$

$$NH_2CH_3 + HCl \xrightarrow{200–300°C} NH_3 + CH_3Cl,$$

$$NH_3 + HCl = NH_4Cl.$$

After the addition of aqueous hydrochloric acid to DMF ([DMF]/[HCl] = 10 : 1), the ^{1}H NMR spectrum of the mixture showed resonances from DMF (δ_{CH} = 7.99 ppm, δ_{CH_3} = 2.75 and 2.91 ppm) and signals at 9.15, 8.17, 5.49, and 2.58 ppm. The resonance signals from the proton of the NH group of secondary amines are known to occur in the 1.2–2.0 ppm range; the resonances from the protons at the nitrogen atom in disubstituted ammonium salts, in the 9–10 ppm range [22]. The appearance of a positive charge on the nitrogen atom causes a downfield shift of both the signals from the NH_2 group and the signals from the methyl (methylene) protons at the nitrogen atom. The signals observed at 9.15 and 2.58 ppm in the ^{1}H NMR spectrum are due to the protons of disubstituted ammonium salts (δ_{NH_2} = 9.15 ppm, δ_{CH_3} = 2.58 ppm) [21], and the signal at δ = 8.17 ppm is due to the aldehyde proton of formic acid.

The heat treatment at 400°C of the salt $[NH_2(CH_3)_2]^+Cl^-$, which is obtained by reacting an aqueous solution of dimethylamine with an equivalent amount of hydrochloric acid, causes its decomposition yielding ammonium chloride, according to X-ray diffraction data. This chemical simulation corroborates the above hypothesis.

Thus, the radical difference between $PdCl_2$ hydrogenolysis and the hydrogenolysis of the oxygen-containing precursors is the formation of a strong acid in the former case. As a consequence, the reduction of palladium dichloride by hydrogen in DMF is accompanied by the catalytic hydrolysis of the solvent followed by the formation of dimethylammonium chloride. With $PdCl_2$ as the precursor, not only the high rate of $PdCl_2$ reduction by hydrogen, but also the appearance of the $[NH_2(CH_3)_2]^+Cl^-$ salt in the reaction system is favorable for the formation of finer palladium black in the DMF medium and for the changes in its supramolecular structure. This is the main cause of the higher catalytic activity and stability of the Pd black forming from $PdCl_2$ as compared to the palladium blacks forming from the oxygen-containing precursors $Pd(acac)_2$ and $Pd(OAc)_2$ in a hydrogen atmosphere.

As was mentioned above, the introduction of elemental phosphorus before the $PdCl_2$ reduction stage decreases the activity of the catalyst in styrene hydrogenation, making it lower that the activity of the $PdCl_2$-based Pd black and the activity of the PdX_2–0.3P (X = acac, OAc) catalytic systems. At the same time, this increases the TON of the catalyst. Earlier, based on the totality of relevant experimental evidence (detection of nanoparticles in the solution, an extremum in the hydrogenation rate as a function of the catalyst concentration, and poisoning of the catalyst by mercury [23]), we deduced that the catalyst in the $Pd(acac)_2$–0.3P system is microheterogeneous. The promoting effect of elemental phosphorus on this system is mainly due to the formation of a finer catalyst [23]. The following model of a nanoparticle of this catalyst was suggested: the core of the particle is formed by Pd_6P, and its shell is made up of Pd(0) clusters, which are active in hydrogenation reactions, are accessible to the coordinating substrate, and can activate it. The inhibiting action of phosphorus in the $Pd(acac)_2$–P system at P/Pd > 0.75 is due to the change in the composition of the catalyst nanoparticles and the decrease in the proportion of Pd(0) because of its conversion into the palladium phosphides Pd_5P_2 and PdP_2 [23].

In order to understand why elemental phosphorus exerts different effects on the properties of palladium catalysts obtained from different precursors, we studied the products of the reaction between palladium dichloride and elemental phosphorus at different stages of catalyst formation, specifically, the reaction in an argon atmosphere and subsequent conversions in a hydrogen atmosphere.

Palladium dichloride reacts readily with white phosphorus at room temperature. Immediately after the addition of elemental phosphorus to a DMF solution of palladium dichloride in an inert atmosphere, the color of the solution changed from orange to black.

Table 2. Products of the interaction of $PdCl_2$ and $Pd(acac)_2$ with white phosphorus in DMF in an inert atmosphere (Pd concentration of 7.0 mmol/l, 20°C)

Precursor	Sample no.	P/Pd	HCl or acac yield, %	Product composition according to X-ray diffraction data
$PdCl_2$	1	0.3	34	Pd_6P, Pd_5P_2, Pd_3P, NH_4Cl
	2	1.0	84	$Pd_{12}P_{3.2}$, $Pd_{4.8}P$, Pd_3P, Pd_5P_2, NH_4Cl
	3	3.0	90	PdP_2, NH_4Cl
$Pd(acac)_2$ [23]	4	0.3	10	PdP_2, Pd_5P_2
	5	1.0	30	PdP_2, Pd_5P_2
	6	3.0	99	Not determined

Hydrochloric acid, phosphorous acid (^{31}P NMR: δ = 4.4 ppm, J_{P-H} = 640 Hz), and phosphoric acid (^{31}P NMR: δ = 3.4 ppm) were identified among the reaction products in the solution. The hydrochloric acid yield measured by potentiometric titration varied between 34% for P/Pd = 0.3 and 84% for P/Pd = 1.0 (Table 2). Note that the conversion of palladium dichloride in its reaction with elemental phosphorus in an argon atmosphere was 3 time higher than the conversion of palladium bisacetylacetonate. The composition of the products indicates that a redox reaction between $PdCl_2$ and white phosphorus takes place in the system, involving water present in the solvent. The same result was obtained for the reaction between palladium bisacetylacetonate and white phosphorus in the presence of D_2O [24].

P_4 is known to be a reductant, and its redox reactions with compounds of transition metals in high oxidation states can yield both metals [25] and metal phosphides [26]. For identification of the products of the reaction between palladium dichloride and elemental phosphorus, the samples isolated from the $PdCl_2$–P reaction system (P/Pd = 0.3, 1.0, 3.0) were characterized by X-ray diffraction. All samples turned out to be X-ray-amorphous. However, the diffuse halo in the diffraction patterns of the samples with P/Pd = 0.3 (sample 1) and P/Pd = 1.0 (sample 2) was observed in the $2\theta = 35°–45°$ range, which accommodate the strongest diffraction peaks from palladium metal and from palladium-rich palladium phosphides (Pd_6P, Pd_3P, Pd_5P_2, etc.). In the diffraction pattern of the sample with P/Pd = 3.0 (sample 3), the diffuse halo maximum was observed at $2\theta = 30°$. This is the place where the strongest diffraction peaks from PdP_2 occur. After the samples were crystallized by heat treatment at 400°C, it was demonstrated by X-ray diffraction that sample 1 contains a mixture of Pd_6P, Pd_5P_2, and Pd_3P; sample 2 contains $Pd_{12}P_{3.2}$ (or $Pd_3P_{0.8}$), $Pd_{4.8}P$, Pd_3P, and Pd_5P_2; and sample 3 contains PdP_2 (Table 2). The palladium metal phase was not detected by X-ray diffraction.

Thus, even before $PdCl_2$ reduction with hydrogen, part of the palladium dichloride, depending on the P/Pd ratio, reacts with elemental phosphorus in an argon atmosphere to yield palladium phosphides, whose formation can be described in terms of the following consecutive–parallel reactions:

$$3PdCl_2 + 2P + 6H_2O = 3Pd(0) + 6HCl + 2H_3PO_3,$$
$$2Pd + P_4 = 2PdP_2,$$
$$PdP_2 + 4Pd = Pd_5P_2,$$
$$Pd_5P_2 + Pd = 2Pd_3P,$$
$$Pd_3P + 3Pd = Pd_6P.$$

The fact that the conversion of $PdCl_2$ in its interaction with elemental phosphorus is higher than the conversion of $Pd(acac)_2$ at a given reactant ratio and the formation of palladium-rich phosphides (Table 2) indicate that palladium dichloride is more reactive toward elemental phosphorus than palladium bisacetylacetonate.

The later stages of the formation of the $PdCl_2$–nP (n = 0.3, 1.0) catalytic system in a hydrogen atmosphere result in quantitative $PdCl_2$ conversion. A TEM study of the $PdCl_2$–nP reaction system demonstrated that the reaction of its components with hydrogen yields a microheterogeneous system in which the particle size of the dispersed phase decreases with an increasing elemental phosphorus concentration (Table 1). For example, at P/Pd = 0.3 the system is dominated by particles 3.1 nm in diameter (Fig. 4). The base nanoparticles form a fractal structure, not macroglobules like those present in Pd black. Similar fractal structures are observed at P/Pd = 1.0. The observation of high-contrast particles in the micrographs indicates that these particles are rich in palladium, but does not make clear whether they are palladium nanoclusters of palladium phosphide nanoparticles.

The catalyst samples isolated from the $PdCl_2$–nP–H_2 reaction system at n = 0.3 (sample 4) and n = 1.0 (sample 5) in the DMF medium are X-ray-amorphous, characterized by a diffuse halo at $2\theta = 35°–40°$. As was noted above, this range of diffraction angles accommodates reflections characteristic of palladium metal and palladium phosphides [12]. The CSD size for n = 0.3 and 1.0 is 3.4 and 1.8 nm, respectively (Table 1). As samples 4 and 5 and Pd black are heat-

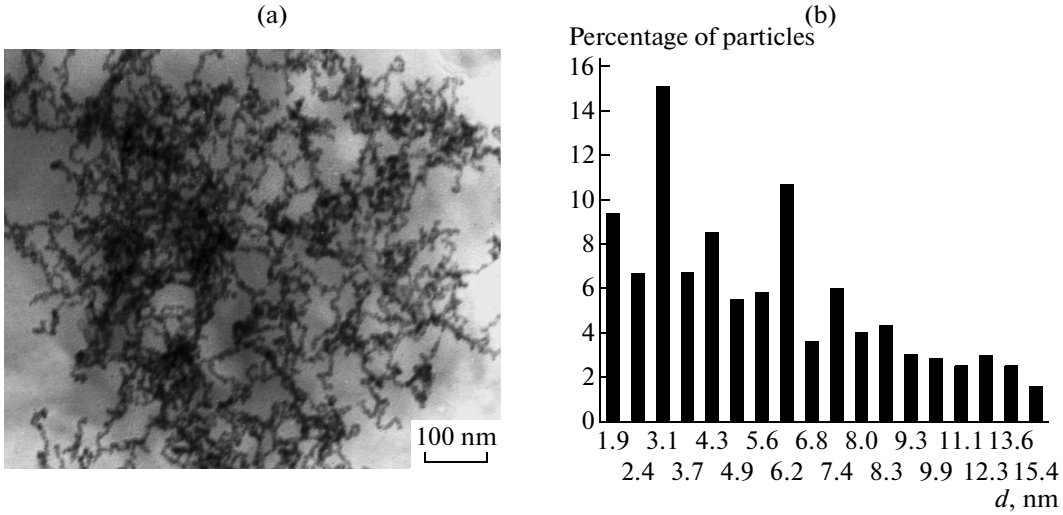

Fig. 4. (a) TEM image of the $PdCl_2$–0.3P system after reduction with hydrogen in the DMF medium (Pd content of 1 mmol/l, 30°C, H_2 pressure of 1 atm). (b) Particle size distribution.

treated at 400°C, part of the material sublimes to yield ammonium chloride.

The diffraction pattern of sample 1, which was prepared in hydrogen at P/Pd = 0.3, shows reflections from crystalline palladium and Pd_6P. According to chemical analysis, the Pd(0) content of sample 1 is 38%.

As was noted above, at P/Pd = 1.0 over 80% of the $PdCl_2$ is converted even in an inert atmosphere via the redox reaction with white phosphorus. Sample 2, which was isolated from the $PdCl_2$–P (P/Pd = 1.0) reaction system treated with hydrogen, contains crystalline palladium along with the palladium phosphides $Pd_{12}P_{3.2}$ and $Pd_{4.8}P$, which also result from the interaction between palladium dichloride and white phosphorus in argon. According to X-ray diffraction data, the Pd(0) content of sample 2 is approximately 3 times lower than that of sample 1. This is in agreement with the results of chemical analysis (Table 1). The formation of the crystalline palladium phase in the $PdCl_2$–nP–H_2 (n = 0.3, 1.0) system distinguishes this system radically from the $Pd(acac)_2$-based catalysts [23].

The difference between the compositions of the phosphides obtained in an inert atmosphere and in hydrogen at the same P/Pd ratio (n = 0.3) suggests that, as the catalyst forms in a hydrogen atmosphere, the palladium phosphide nanoparticles react further with Pd(0) atoms resulting from hydrogenolysis to yield palladium-rich phosphides.

An analysis of the above data demonstrates that modifying the $PdCl_2$-based catalyst with elemental phosphorus causes a decrease in the nanoparticle size and, at the same time, diminishes the proportion of reduced palladium because of the formation of palladium phosphides. The detection of the palladium metal phase along with the palladium phosphides is evidence that, owing to the high $PdCl_2$ reduction rate and, as a consequence, high supersaturation, the Pd(0) atoms forming in the hydrogen atmosphere react not only with the palladium phosphides, yielding palladium-rich phosphide (Pd_6P) nanoparticles, but also with one another. Thus, both homogeneous and heterogeneous nucleation of Pd clusters takes place. The homogeneous nucleation followed by nucleus growth yields palladium nanoclusters. In the heterogeneous nucleation of Pd(0) clusters, the palladium phosphide particles present in the solution can serve as crystallization centers. This mechanism favors the formation of core–shell nanoparticles consisting of a Pd_6P core and palladium clusters on its surface. The above data suggest that $PdCl_2$ reduction with hydrogen in the presence of elemental phosphorus can yield palladium phosphide nanoparticles and palladium nanoclusters and do not rule out the formation of core–shell particles (scheme).

The formation of palladium nanoclusters, which are smaller than Pd black particles, and the formation of Pd_6P core–Pd_x shell nanoparticles, whose hydrogenation-active surface Pd(0) atoms are accessible to coordinating substrate molecules and hydrogen, do not provide explanation for the inhibiting effect of elemental phosphorus. The fact of inhibition itself suggests a decrease in the proportion of hydrogenation-active Pd(0) clusters. This can be due to the conversion of a greater part of palladium into hydrogenation-inactive palladium phosphides, which is actually observed as the P/Pd ratio is raised, and to the partial poisoning of the Pd(0) clusters by chloride ions from the $[NH_2(CH_3)_2]Cl$ salt. This is indicated by the fact that the Pd black obtained from palladium dichloride is less active than the $Pd(acac)_2$–0.3P–H_2 system at comparable nanoparticle diameters. Further evidence of the inhibiting effect of the chloride ions on the nanosized palladium catalysts modified with elemen-

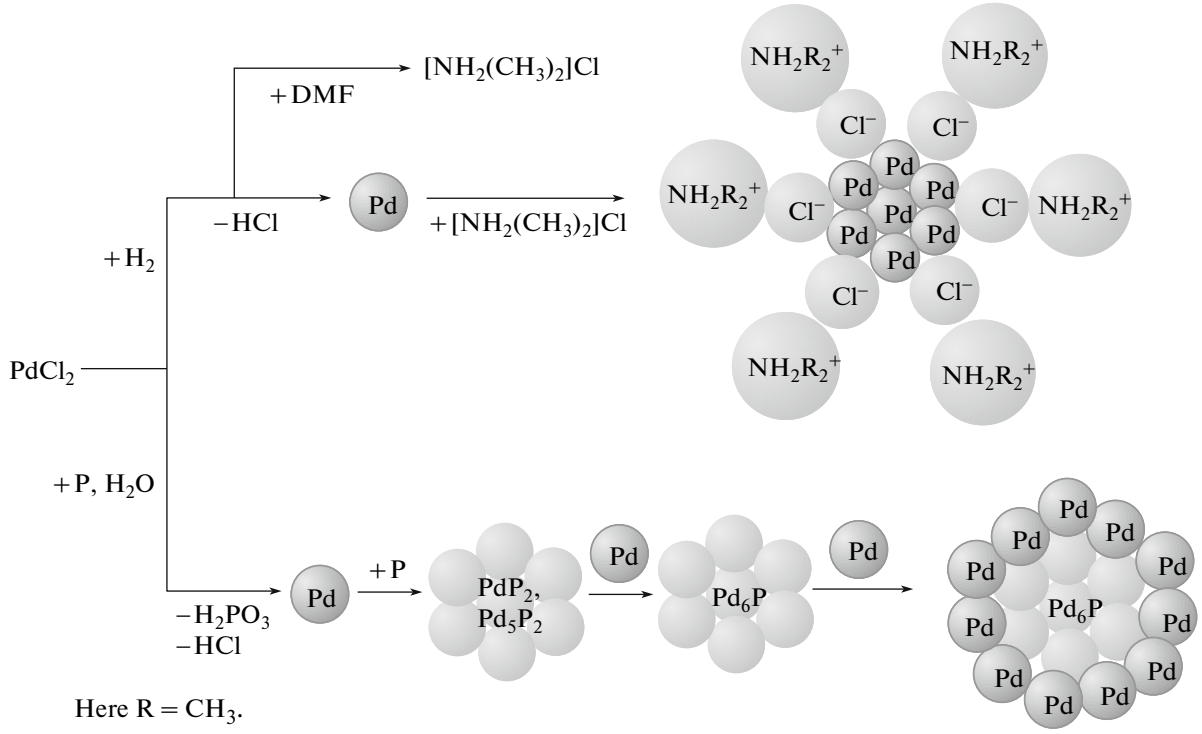

Scheme.

tal phosphorus was provided by experiments in which ammonium chloride was introduced into the $Pd(acac)_2$–0.3P catalytic system. At $NH_4Cl/Pd = 0.5$, the catalytic activity of this system in styrene hydrogenation is lower by 12%; at $NH_4Cl/Pd = 1.0$, by 50%.

Thus, the effect of the nature of the acido ligand in the precursor on the properties of the palladium catalysts modified with elemental phosphorus is determined by at least two factors, namely, the rate of reduction of the Pd(II) compound by hydrogen and the nature of the resulting acid. The difference between the reactivities of the Pd(II) compounds toward hydrogen and elemental phosphorus can lead both to the formation of segregated palladium nanoclusters and palladium phosphide nanoparticles and to the formation of core–shell nanoparticles. The introduction of an acid can bring about the catalytic decomposition of the solvent (DMF) as a side process.

ACKNOWLEDGMENTS

This work was carried out in the framework of the Federal Purpose-Oriented Program "Scientific and Pedagogical Cadre of Innovative Russia" (state contract no. P 1344).

REFERENCES

1. Boreskov, G.K., *Geterogennyi kataliz* (Heterogeneous Catalysis), Moscow: Nauka, 1986.
2. Navalikhina, M.D. and Krylov, O.V., *Usp. Khim.,* 1998, vol. 67, p. 657.
3. Molnar, A., Sarkany, A., and Varga, M., *J. Mol. Catal. A: Chem.*, 2001, vol. 173, p. 185.
4. Bonnemann, H. and Richards, R.M., *Eur. J. Inorg. Chem.*, 2001, p. 24552.
5. Nagaveni, K., Gayen, A., Subbanna, G.N., and Hegde, M.S., *J. Mater. Chem.*, 2002, vol. 12, p. 3147.
6. Ito, K., Ohshima, M., Kurokawa, H., Sugiyama, K., and Miura, H., *Catal. Commun.*, 2002, no. 3, p. 527.
7. RF Patent 2323776, 2008.
8. Gordon, A.J. and Ford, R.A., *A Handbook of Practical Data, Techniques, and References*, New York: Wiley, 1972.
9. Mitchell, J. and Smith, D., *Aquametry,* New York: Plenum, 1977.
10. US Patent 3474464, 1969.
11. Kitaigorodskii, A.I., *Rentgenostrukturnyi analiz* (X-ray Crystallography), Moscow: Tekhteorizdat, 1950.
12. *Powder Diffraction File, Hanawalt Search Manual: Inorganic Phases*, Swarthmore: Joint Committee on Powder Diffraction Standards, 1992, sets 1–42.
13. Boone, S. and Kleppa, O.J., *J. Chem. Thermodyn.*, 1991, vol. 23, p. 1147.
14. Wiehage, G., Weibke, Fr., and Biltz, W., *Z. Anorg. Allg. Chem.*, 1936, vol. 228, p. 357.
15. Shmidt, A.F. and Mametova, L.V., *Kinet. Katal.,* 1996, vol. 37, no. 3, p. 431 [*Kinet. Catal.* (Engl. Transl.), vol. 37, no. 3, p. 406].
16. Belykh, L.B., Skripov, N.I., Belonogova, L.N., Umanets, V.A., and Shmidt, F.K., *Zh. Prikl. Khim.*, 2007,

vol. 80, p. 1489 [*Russ. J. Appl. Chem.* (Engl. Transl.), vol. 80, p. 1523].

17. Pomogailo, A.D., Rozenberg, A.S., and Uflyand, I.E., *Nanochastitsy metallov v polimerakh* (Metal Nanoparticles in Polymers), Moscow: Khimiya, 2000.
18. Shmidt, F.K., *Fraktal'nyi analiz v fiziko-khimii geterogennykh sistem i polimerov* (Fractal Analysis in the Physical Chemistry of Heterogeneous Systems and Polymers), Irkutsk: Irkutsk. Gos. Univ., 2001.
19. Zhang, J., Keita, B., Nadjo, L., Mbomekalle, I.M., and Liu, T., *Langmuir,* 2008, vol. 24, p. 5277.
20. *Khimicheskaya entsiklopediya* (Encyclopedia of Chemistry), Knunyants, I.L., Ed., Moscow: Sovetskaya Entsiklopediya, 1990, vol. 2.
21. Karrer, P., *Lehrbuch der organischen Chemie*, Stuttgart: Georg Thieme, 1959.
22. *Spectral Database for Organic Compounds (SDBS)*, National Institute of Advanced Industrial Science and Technology, http://riodb01.ibase.aist.go.jp/sdbs/cgi-bin/cre_index.cgi?lang=eng.
23. Skripov, N.I., *Cand. Sci. (Chem.) Dissertation*, Irkutsk: Irkutsk State Univ., 2007.
24. Belykh, L.B., Skripov, N.I., Belonogova, L.N., Rokhin, A.V., and Shmidt, F.K., *Zh. Obshch. Khim.*, 2009, vol. 79, p. 94 [*Russ. J. Gen. Chem.* (Engl. Transl.), vol. 79, p. 92].
25. Dorfman, Ya.A., Aleshkova, M.M., Polimbekova, G.S., Levina, L.V., Petrova, T.V., Abdreimova, R.R., and Doroshkevich, D.M., *Usp. Khim.,* 1993, vol. 62, p. 928.
26. Nekrasov, B.N., *Osnovy obshchei khimii* (Fundamental General Chemistry), Moscow: Khimiya, 1974, vol. 1.